

Systematic Model Builder, Model-Based Design of Experiments, and Design Space Identification for A Multistep Pharmaceutical Process – Toward Quality by Digital Design

Xuming Yuan^a, Ashish Yewale^a, Brahim Benyahia^{a*}

^a Loughborough University, Department of Chemical Engineering, Epinal Way, Loughborough, Leicestershire, LE11 3TU, UK

* Corresponding Author: B.Benyahia@lboro.ac.uk.

ABSTRACT

This study aims at developing a holistic approach to establish robust mathematical models of integrated and interactive multistep processes, while systematically identifying the corresponding design space and acceptable operating region (AOR). The overall objective is to reduce the experimentation costs, enhance accuracy of integrated mathematical models, and deliver built-in quality assurance based on a new Quality by Digital Design (QbDD) paradigm. This methodology starts with the construction of a set of model candidates for different unit operations, based on the prior knowledge and inherent assumptions. Several model candidates of the integrated multistep process are considered. A model discrimination based on model prediction performance reveals the best integrated model for the multistep process. In the next step, the estimability analysis and model-based design of experiment (MBD_{oE}) are implemented to deliver information-rich data and systematically refine the integrated model. With the acquisition of the new experimental data, the reliability and robustness of the multistep mathematical model is dramatically enhanced. A blending-tableting process is considered to validate the methodology. The model captures the effects of the blender as well as the composition and porosity of the tablet on the tablet tensile strength. Model discrimination and automated model refinement are then performed to identify and improve the optimal integrated model for this two-step process, and the enhanced model is applied for the design space identification under specified CQA targets and associated bounds.

Keywords: Multistep process, Model builder, Model Based DoE, Design Space, Acceptable Operating Region (AOR), Quality by Digital Design (QbDD), Blending, Tableting.

1. INTRODUCTION

The mathematical models of different processing units within a manufacturing process or plant are usually established and optimized individually, even when these processes are sequentially combined in the real world, particularly in continuous operating plants. Although this traditional modeling approach may help reduce complexity, it can lead to suboptimal solutions or/and overlook the interactions between the unit operations, which also potentially increase the development time, wastes, and experimental costs inherent to the raw materials, solvents, cleaning, etc.

The quality assurance of pharmaceutical products is

traditionally performed through Quality-by-Testing (QbT), which is an experiment-intensive a-posteriori approach, leading to poor flexibility and higher failure risks. The advent of Quality-by-Design (QbD) has opened new avenues to adapt more effective risk-based quality management methods in Pharma. Nonetheless, current applications of QbD are still heavily reliant on expensive designs of experiments (DoE) and driven by data intensive methodologies.

As required in QbD, the quality assurance of pharmaceutical product must be built-in from the development phase and throughout the life cycle, where the critical quality attributes (CQAs) of the product should be always satisfied during manufacturing. This requirement

may be effectively driven by mathematical models and digital tools which must exhibit higher levels of reliability and prediction capabilities. Additionally, the robustness of the mathematical models can play a vital role in identification of robust design space and cost-effective operating/control strategies in QbD [2]. However, the traditional approaches for the construction of reliable and predictive mathematical models can be labour-intensive, resource-demanding and time-consuming, which is often not an available option, especially at the early stage of process development where the availability of large quantities of active pharmaceutical ingredients (APIs) may be compromised by the lack of scalable units. Another challenge comes from the competition of multiple model candidates originating from different assumptions of the system behaviour, where the lack of identifiability of the model parameters exacerbates the problem and result in unreliable models or poor prediction performance. Importantly, the mathematical models of individual units are commonly developed with the risk of overlooking or neglecting the interactions between unit operations in a complete pharmaceutical process.

One potential solution to address these challenges lies in the improvement of the experimental designs, based on which the data for model calibration are acquired. The information content and the cost-efficiency of different experimental designs can vary significantly. Standard DoE techniques are commonly applied in traditional methods, which may become cost prohibitive for complex systems due to the unrealistically high number of required experiments [8]. Moreover, they are not necessarily optimally designed in terms of obtaining information content for model calibration. Hence, model-based design of experiment (MBD_{oE}) emerges as an effective solution offering enhanced flexibility, maximized information content, and reduced experimental costs.

Here, our proposed methodology extends the MBD_{oE} capabilities to multistep integrated or interactive processes [11]. The approach is further enhanced by incorporating effective capabilities for systematic model discrimination and estimability analysis, followed by a model-based identification of robust design space and acceptable operating region (AOR), laying the ground for novel Quality by Digital Design (QbDD) paradigms.

2. METHODS

The proposed holistic methodology is outlined in Figure 1, which upgrades the capabilities of the previously presented framework to the case of multiple processes and design space identification [11]. Since various assumptions can be applied at the early stage of process development, this approach begins with the construction of model candidates for different unit operations, which are then combined to give a series of integrated models for the complete process. Instead of evaluating the model candidates of each unit independently, parameter estimation and model discrimination will focus on the integrated models, thus the risk of omitting the interactions between different units is inherently reduced. The parameter estimation can utilize the prior knowledge of the system if available (e.g., previous experimental data, nominal values of parameters), as well as the preliminary experimental data. Afterwards, the model discrimination is conducted through the computation of the Akaike information criterion (AIC) [1] of each model candidate, where the model with the lowest AIC value is the best in capturing the system feature with the lowest model complexity. Subsequently, the automated model refinement is initiated with the estimability analysis by applying sequential orthogonalization algorithm [9] using a threshold value of 0.1 on the best integrated model, which identifies the estimable parameter subset. It should be noted that

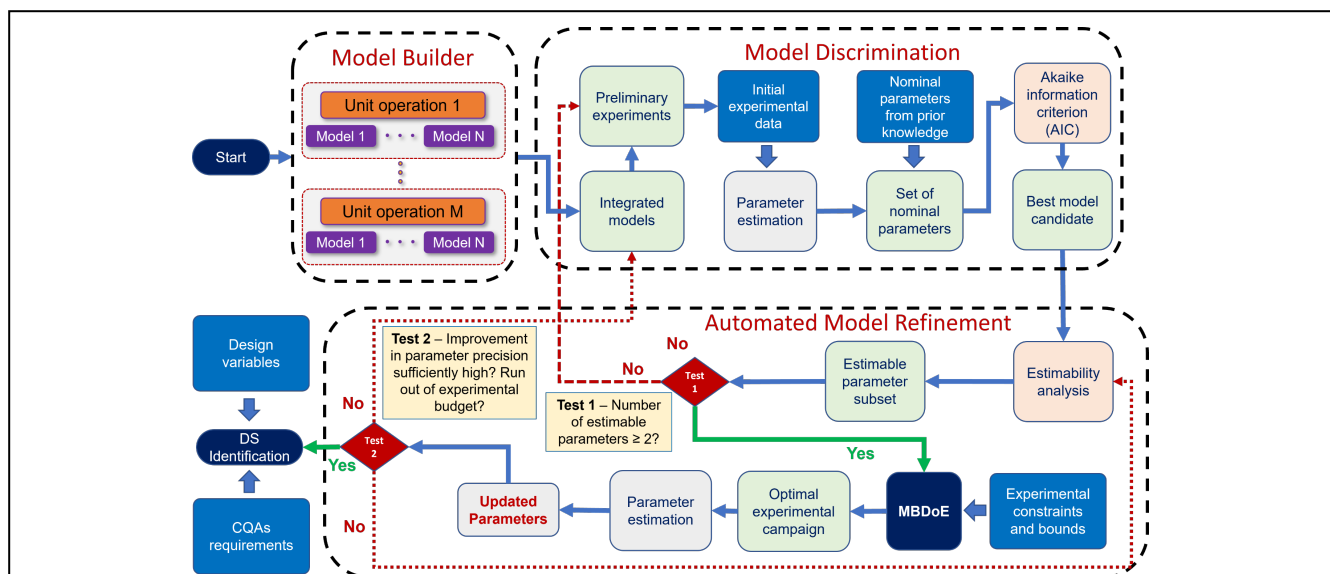


Figure 1: Proposed method for model building, discrimination, automated refinement & design space identification

extremely low information content in the preliminary experimental data can lead to a very small number of estimable parameters (less than two) (Test 1), thus extra preliminary experimental runs are required, or alternatively another integrated model may be selected. Once Test 1 is passed, MBDofE focusing on the Fisher information matrix (FIM) of the estimable parameter subset is performed, where the new experimental data are utilised to update the parameter estimates and uncertainties. The model refinement workflow can be executed automatically until the improvement of the parameter precision becomes insignificant, or the experimental budget is depleted (Test 2). Once the stopping criterion is triggered, the automated model refinement procedure is terminated, and the design space identification based on the enhanced process model is performed, where the best nominal operating point (NOP) and the corresponding acceptable operating region (AOR) are identified, delivering a multi-dimensional space where the variations of the critical process parameters (CPP) meet the CQAs requirements.

3. CASE STUDY

A two-step blending-tableting process was investigated to validate the proposed holistic framework. The preliminary data or prior knowledge was obtained from the literature [4]. In blending-tableting system, the tablet composition can be varied by changing the weight fraction of the lubricant (magnesium stearate, MgSt) and three different diluents MCC Avicel PH102, Fast Flo Lactose 316 and dibasic calcium phosphate (we will denote them as MCC, LAC and DCP), while the lubrication is conducted by blending the powder in TURBULA® blenders, where the size and headspace fraction of the blender and the number of blending cycles can vary. There are 143 experimental runs available from the literature [4] with different compositions, porosity and blender settings.

3.1 Model equations

For blending and tableting processes, several models were proposed in [3], [5] and [6] to capture the dependence of the tablet tensile strength on either the tablet porosity, composition, or the blender operating variables. The model proposed in [3] consists of Equations 1 to 3, where σ_0 is the tablet tensile strength at zero porosity, σ_{nobld} denotes the tensile strength before blending, ε refers to tablet porosity, k_b represents bonding capacity, k refers to lubrication extent, α_b , V_b , F_h , ω_b , t_b are the equipment dependent factor, volume, headspace fraction, rotation speed and blending time of the blender, β signifies lubrication sensitivity, γ is the lubrication rate constant of the blend, and σ is the final tensile strength.

$$\sigma_{nobld} = \sigma_0 \exp(-k_b \varepsilon) \quad (1)$$

$$k = \alpha_b V_b^{\frac{1}{3}} F_h \omega_b t_b \quad (2)$$

Table 1: Comparison of blending-tableting models proposed in [3], [5] and [6].

Model	Porosity	Composition	Blending
[3]	Eq. 1	N/A	Eq. 2 and 3
[5]	Eq. 4 or 5	N/A	Eq. 2 and 3
[6]	Eq. 1	Eq. 6 and 7	Eq. 8

$$\sigma = \sigma_{nobld} [(1 - \beta) + \beta \exp(-\gamma k)] \quad (3)$$

Equation 1 is commonly referred as Ryshkewitch equation which capture the interdependence between tablet tensile strength and porosity. With Equations 2 and 3, the effects of the blender features and the operating variables are captured. Compared with [3], [5] directly linked the lubrication sensitivity β with the porosity ε with linear/exponential assumptions, resulting in Equations 4 or 5, where a_1 and a_2 are the parameters to be estimated. The blender effects are modelled with the same equations (2 and 3) in [5].

$$\beta = a_1 \varepsilon + a_2 \quad (4)$$

$$\beta = a_1 \exp(-a_2 \varepsilon) \quad (5)$$

The main limitation of the models in [3] and [5] is the lack of tablet composition effects. Thus, the model developed in [6] simulated the effect of weight fraction changes of the lubricant and diluent, where the bonding capacity k_b of the mixed powder is depends on the ratio of the specific surface area between the lubricant and diluent ($S_{lub/dil}$), which is calculated by Equation 6, where the specific surface area of the lubricant and diluent $S_{BET,lub}$ and $S_{BET,dil}$ as well as their weight fractions w_{lub} and w_{dil} are used. Afterwards, k_b is obtained in Equation 7, where κ is the coefficient corresponding to $S_{lub/dil}$, and $k_{b,dil}$ is the bonding capacity of diluent.

$$S_{lub/dil} = \frac{S_{BET,lub} w_{lub}}{S_{BET,dil} w_{dil}} \quad (6)$$

$$k_b = \kappa S_{lub/dil} + k_{b,dil} \quad (7)$$

The effect of tablet porosity is also captured in [6] by Ryshkewitch equation. However, the blender effects are not included. Instead, the tensile strength of the tablet made of the mixed powder at zero porosity is predicted (Equation 8), where $\sigma_{dil,0}$ is the tensile strength of the tablet only made of the diluent at zero porosity.

$$\sigma_0 = \sigma_{dil,0} \exp(-\beta S_{lub/dil}) \quad (8)$$

Table 1 summarizes the models proposed in [3], [5] and [6]. All models capture the effect of tablet porosity. Only [6] models the effect of composition, but [3] and [5] are more comprehensive in modelling the blender effects. Therefore, there is an opportunity to build a more sophisticated integrated model for this process.

3.2 Set of multistep model candidates

With the aim of capturing the effect of tablet porosity, composition and the blender by adapting the model

equations in [3], [5] and [6], four candidates of the blending-tableting process are constructed, where Equation 1 is applied in all the candidates to model the influence of porosity, while the blender effects are simulated by Equations 2 and 3. The main adaptation focuses on the composition. In [6], the equations were developed for a single lubricant – single diluent tablet system, while the system in [4] involves one lubricant and three diluents. Therefore, we first propose the equations calculating the tensile strength of the tablet made of mixed diluents at zero porosity ($\sigma_{dil,0}$), where linear assumption (Equation 9) and exponential assumption (Equation 10) of $\sigma_{dil,0}$ on the weight fraction of each diluent ($w_{dil,i}$) are adopted. In Equation 9, $\sigma_{dil,i,0}$ is the tensile strength of the tablet only made of diluent i at zero porosity; in Equation 10, $\sigma_{dil,0,max}$ is the maximum tensile strength of the tablet made of the mixture of the diluents that can be achieved at zero-porosity; p_i are the parameters to weigh the contribution of different diluents on $\sigma_{dil,0}$.

$$\sigma_{dil,0} = \sum_{i=1}^n p_i w_{dil,i} \sigma_{dil,i,0} \quad (9)$$

$$\sigma_{dil,0} = \sigma_{dil,0,max} [1 - \exp(-\sum_{i=1}^n p_i w_{dil,i})] \quad (10)$$

Inspired by [5], we assume the lubrication sensitivity β to be linearly/exponentially dependent on $S_{lub/dil}$ (Equation 11/12), while $S_{lub/dil}$ is assumed to be the ratio of the weighted sum of the specific surface area of the lubricant and diluent (Equation 13), and the bonding capacity k_b is also assumed to be relevant to the weighted sum of the bonding capacity of each diluent (Equation 14). The candidates of integrated models are summarized in Table 2.

$$\beta = a_1 S_{lub/dil} + a_2 \quad (11)$$

$$\beta = a_1 \exp(-a_2 S_{lub/dil}) \quad (12)$$

$$S_{lub/dil} = \frac{\sum_{i=1}^m S_{BET,lub,i} w_{lub,i}}{\sum_{j=1}^n S_{BET,dil,j} w_{dil,j}} \quad (13)$$

$$k_b = \kappa S_{lub/dil} + \sum_{j=1}^n k_{b,dil,j} w_{dil,j} \quad (14)$$

The data in [4] are divided into two groups randomly for parameter estimation (70%) and validation (30%). Once the best integrated model is identified, automated model refinement will be performed, minimizing the dimensionless normalized confidence ellipsoid volume of the estimable parameter subset $V_{est,norm,dimless}$. This first requires the computation of the sensitivity matrix Z of the model parameters (Equation 15), where $\sigma_{exp,i}$ refers to the tablet tensile strength obtained from experiment i , while θ_j denotes the j th model parameter. Then the FIM of the integrated model is computed by Equation 16. Let FIM_0 be the FIM of the parameters calculated with the preliminary experimental data (the data from [4]), its diagonal entries D_0 (Equation 17) is used to normalize the

Table 2: Proposed model candidates of the integrated blending-tableting process

Model	Porosity	Composition	Blending
1		Eq. 9, 11, 13 and 14	
2	Eq. 1	Eq. 9, 12, 13 and 14	Eq. 2 and 3
3		Eq. 10, 11, 13 and 14	
4		Eq. 10, 12, 13 and 14	

FIM (Equation 18), and the normalized FIM of the estimable parameter subset ($FIM_{est,norm}$) is its sub-matrix by extracting the rows and columns of corresponding to the estimable parameters. Finally, as the number of the estimable parameters N_{est} can change at each MBDoE cycle in the automated model refinement, $V_{est,norm,dimless}$ is calculated based on Equation 19, which is in essence a normalized form of the D-optimal criterion.

$$Z = \begin{bmatrix} \frac{\partial \sigma_{exp1}}{\partial \theta_1} & \dots & \frac{\partial \sigma_{exp1}}{\partial \theta_N} \\ \vdots & \ddots & \vdots \\ \frac{\partial \sigma_{expM}}{\partial \theta_1} & \dots & \frac{\partial \sigma_{expM}}{\partial \theta_N} \end{bmatrix} \quad (15)$$

$$FIM = Z^T Z \quad (16)$$

$$D_0 = \text{diag}(FIM_0) \quad (17)$$

$$FIM_{norm} = D_0^{-\frac{1}{2}} FIM D_0^{-\frac{1}{2}} \quad (18)$$

$$V_{est,norm,dimless} = \left(\sqrt{\det(FIM_{est,norm}^{-1})} \right)^{\frac{1}{N_{est}}} \quad (19)$$

In each automated model refinement cycle, the MBDoE procedure presented by Equation 20 is conducted to identify the optimal experimental design that minimizes parameter uncertainties, where the decision variables include the volume (V_b) and headspace fraction (F_h) of the blender, blending cycles (N_b), mass fractions of MgSt (w_{MgSt}), MCC (w_{MCC}) and LAC (w_{LAC}), and the tablet porosity (ε). The mass fraction of DCP acts as a constraint that should lie between 0% and 100%.

$$\begin{aligned} & \min_{V_b, F_h, N_b, w_{MgSt}, w_{MCC}, w_{LAC}, \varepsilon} V_{est,norm,dimless} \\ & \text{s.t. } V_b = \{30\text{mL}, 1250\text{mL}\} \\ & \quad 30\% \leq F_h \leq 70\% \\ & \quad 24 \leq N_b \leq 190512 \\ & \quad 0.5\% \leq w_{MgSt} \leq 2\% \\ & \quad 0\% \leq w_{MCC} \leq 100\% \\ & \quad 0\% \leq w_{LAC} \leq 100\% \\ & \quad 5\% \leq \varepsilon \leq 30\% \\ & \quad 0\% \leq 1 - w_{MgSt} - w_{MCC} - w_{LAC} \leq 100\% \end{aligned} \quad (20)$$

The stopping criteria of the automated model refinement are presented in Equations 21 and 22. Equation 21 captures the relative reduction in the overall parameter uncertainties over a consecutive MBDoE cycles. If the improvement of parameter precision is not sufficiently high between the two consecutive MBDoE cycles, the automated model refinement will be stopped. Equation 22

defines the available experimental budget which represents a maximum of 5 MBDoE cycles in this case.

$$\eta_i = \frac{V_{est, norm, dimless, i-1} - V_{est, norm, dimless, i}}{V_{est, norm, dimless, i-1}} \leq 10\% \quad (21)$$

$$N_{exp, budget} = 5 \quad (22)$$

Once the automated model refinement is completed, a model-based risk assessment is conducted to identify the set of critical process parameters (CPPs) and critical material attributes (CMAs) [10], then followed by a model-based identification of the design space and normal operating range of the blending-tableting process. The CQA bounds are captured by the constraints in Equation 23, which specifies that the tablet tensile strength should be at least 4 MPa with $\geq 85\%$ probability, where Equation 24 summarizes the design variables x . The design space identification is performed with the Python-based tool DSIDE [7], and all the computation is performed on a 11th Gen Intel(R) Core (TM) i5-11400 @ 2.60GHz 2.59 GHz CPU with 16GB RAM.

$$DS = \{x \in X | E[Pr(\sigma \geq 4MPa) | \theta] \geq 85\% \} \quad (23)$$

$$x = [V_b, F_h, N_b, w_{MGSt}, w_{MCC}, w_{LAC}, \epsilon] \quad (24)$$

4. RESULTS & DISCUSSION

The parameter estimation and model discrimination of the four model candidates was conducted. Figure 2 shows the parity plots of the candidates comparing the model prediction with the experimental data, revealing that Models 3 and 4 outperform Models 1 and 2, thus the exponential assumption (Equation 10) outperforms the linear assumption (Equation 9) for $\sigma_{dil,0}$. Since Model 3 has the lowest AIC value (Table 3), it is the best candidate in this case study.

The automated model refinement of Model 3 is performed subsequently. Table 4 shows that the number of estimable parameters and overall precision of the model parameters were both improved with the increase of the number of MBDoE cycles. Initially, six parameters were

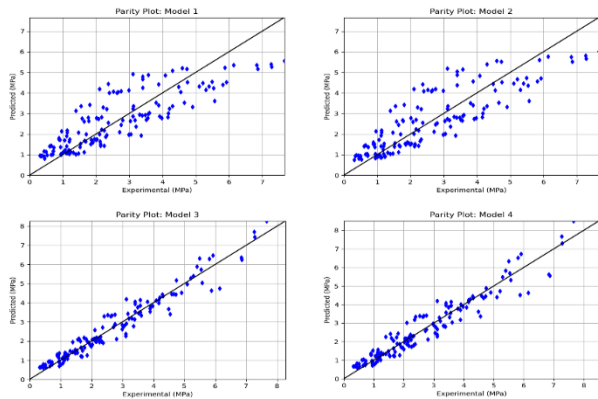


Figure 2. Parity plots (model prediction vs. experimental data) of the candidates. Top left: model 1. Top right: model 2. Bottom left: model 3. Bottom right: model 4.

Table 3: AIC values of the model candidates

Model	1	2	3	4
AIC value	175.51	167.85	47.87	61.24

estimable based on the preliminary data. The 1st MBDoE improved the overall parameter precision (η_i) by 98.68%. In the 2nd MBDoE, η_i significantly dropped (-117.40%), but this is due to the increase of the number of estimable parameters (from 6 to 7), showing that the estimability of the parameters become higher with the new data. With the 3rd, 4th and 5th MBDoE, the overall parameter precision was further enhanced with the increased data size and information content. Since the experimental budget was depleted, the model refinement was terminated.

The improvement in parameter precision can be visualized by the 95% confidence ellipse plots. Figure 3 illustrates the evolution of the joint confidence domain of two selected parameters κ and $k_{b,DCP}$. Over the MBDoE cycles, the nominal estimates are updated, and the confidence ellipse generally becomes smaller, indicating that the knowledge of the model parameters is augmented through the proposed automated model refinement.

After successful model refinement based on the combined estimability and MBDoE, the criticality analysis is conducted to identify the set of CPPs and CMAs based on the approach proposed in [10]. Finally, a design space identification was carried out based on the refined mathematical model and the set of CPPs and CMAs by considering the targeted CQA bounds. To further visualize the improvement of the model, we compared the design space and acceptable operating region (AOR) obtained with the initial model against the refined model. Figure 4 visualizes the design space by the green zones, showing that larger AOR is obtained with the refined model, indicating better operating flexibility and robustness.

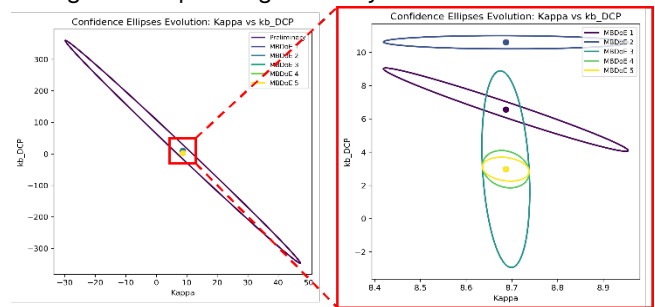


Figure 3. 95% joint confidence ellipses for the parameters κ and $k_{b,DCP}$ after each MBDoE cycle.

Table 4: Improvement of the number of estimable parameters and parameter precision over the MBDoE cycles.

MBDoE	N_{est}	η_i
0 (Preliminary)	6	N/A
1	6	98.68%
2	7	-117.40%
3	7	30.40%
4	7	26.34%
5	7	11.31%

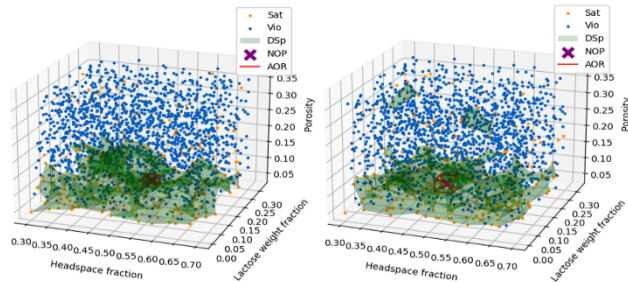


Figure 4. Design space of the blending-tableting process based on the model before (left) and after (right) automated model refinement. Sat: satisfying points. Vio: violating points. DSP: design space. NOP: nominal operating point. AOR: acceptable operating region.

Hence, the proposed holistic framework for model building, discrimination and automated model refinement provides a cost-effective option to establish robust model for the blending-tableting process in this case study, resulting in lower uncertainty and a larger AOR offering enhanced flexibility. The proposed framework constructs a new Quality-by-Digital-Design (QbDD) paradigm offering enhanced capabilities compared to the current Quality-by-Design which heavily relies on expensive designs of experiments and time-consuming costly risk assessment methods. Most importantly, the proposed framework addresses the cases of multistep processes and lay the ground for the implementation of effective QbDD in the integrated pharmaceutical manufacturing.

5. CONCLUSIONS

In this paper, a new integrated approach for model construction, discrimination, automated refinement and design space identification for multistep processes is proposed, which aims at establishing robust mathematical models for the processes involving multiple interactive unit operations in a cost-effective way and laying the ground for a new Quality-by-Digital-Design framework. The validation of the approach on a two-step blending-tableting process has demonstrated the power of the proposed methodology, indicating its potential effectiveness to be extended for wider applications in the development of multistep process models.

ACKNOWLEDGEMENTS

The authors acknowledge funding from the UK Engineering and Physical Sciences Research Council (EPSRC), for Made Smarter Innovation – Digital Medicines Manufacturing Research Centre (DM2), EP/V062077/1.

REFERENCES

1. Akaike, H. A New Look at the Statistical Model Identification. *IEEE Trans. Autom. Control* 1974, 19 (6), 716–723. <https://doi.org/10.1109/tac.1974.1100705>.

2. Benyahia, B.; Anandan, P. D.; Rielly, C. Robust Model-Based Reinforcement Learning Control of a Batch Crystallization Process. In *Proceedings of the 9th ICSC, 2021*, pp 89–94.
3. Kushner, J.; Moore, F. Scale-Up Model Describing the Impact of Lubrication on Tablet Tensile Strength. *Int. J. Pharm.* 2010, 399 (1–2), 19–30. <https://doi.org/10.1016/j.ijpharm.2010.07.033>.
4. Kushner, J. Incorporating Turbula Mixers into a Blending Scale-Up Model for Evaluating the Effect of Magnesium Stearate on Tablet Tensile Strength and Bulk Specific Volume. *Int. J. Pharm.* 2012, 429 (1–2), 1–11. <https://doi.org/10.1016/j.ijpharm.2012.02.040>.
5. Nassar, J.; Williams, B.; Davies, C.; Lief, K.; Elkes, R. Lubrication Empirical Model to Predict Tensile Strength of Directly Compressed Powder Blends. *Int. J. Pharm.* 2021, 592, 119980. <https://doi.org/10.1016/j.ijpharm.2020.119980>.
6. Puckhaber, D.; Finke, J. H.; David, S.; Serratoni, M.; Zafar, U.; John, E.; Juhnke, M.; Kwade, A. Prediction of the Impact of Lubrication on Tablet Compactibility. *Int. J. Pharm.* 2022, 617, 121557. <https://doi.org/10.1016/j.ijpharm.2022.121557>.
7. Sachio, S.; Likozar, B.; Kontoravdi, C.; Papathanasiou, M. M. Computer-Aided Design Space Identification for Screening of Protein A Affinity Chromatography Resins. *J. Chromatogr. A* 2024, 1722, 464890. <https://doi.org/10.1016/j.chroma.2024.464890>.
8. Lackowska, I.; Dragosavac, M. M.; Vladislavljevic, G. T.; Benyahia, B. Production and Tuning of Spherical Agglomerates of Benzoic Acid Using Membrane Dispersion Systems. *Cryst. Growth Des.* 2023, 23 (12), 8897–8908.
9. Benyahia, B.; Latifi, M. A.; Fonteix, C.; Pla, F. Emulsion Copolymerization of Styrene and Butyl Acrylate in the Presence of a Chain Transfer Agent. Part 2: Parameters Estimability and Confidence Regions. *Chem. Eng. Sci.* 2013, 90, 110–118.
10. Campbell, T. J. S.; Rielly, C. D.; Benyahia, B. Digital Design and Optimization of an Integrated Reaction-Extraction-Crystallization-Filtration Continuous Pharmaceutical Process. *Comput.-Aided Chem. Eng.* 2022, 51, 775–780.
11. Yuan, X.; Benyahia, B. A Holistic Approach for Model Discrimination, Multi-Objective Design of Experiment and Self-Optimization of Batch and Continuous Crystallization Processes. *Comput.-Aided Chem. Eng.* 2024, 53, 391–396.

© 2025 by the authors. Licensed to PSEcommunity.org and PSE Press. This is an open access article under the creative commons CC-BY-SA licensing terms. Credit must be given to creator and adaptations must be shared under the same terms. See <https://creativecommons.org/licenses/by-sa/4.0/>

